Hindawi
Wireless Communications and Mobile Computing
Volume 2021, Article ID 7057513, 13 pages
https://doi.org/10.1155/2021/7057513

Research Article

Improved Height Estimation Using Extended Kalman Filter on UWB-Barometer 3D Indoor Positioning System

Ji Li,[1] Yepeng Wang ,[1] Zhuo Chen,[2] Linlin Ma,[3] and Suqing Yan [1,4]

[1] *Guangxi Key Laboratory of Image and Graphic Intelligent Processing, Guilin University of Electronic Technology, Guilin 541004, China*
[2] *University of British Columbia, Vancouver, Canada*
[3] *Zhengzhou Locaris Technology Co., Ltd., Zhengzhou 450000, China*
[4] *Guangxi Key Laboratory of Precision Navigation Technology and Application, Guilin University of Electronic Technology, Guilin 541004, China*

Correspondence should be addressed to Yepeng Wang; yepengwang1@163.com and Suqing Yan; yansuqing@guet.edu.cn

Received 30 April 2021; Revised 19 June 2021; Accepted 1 July 2021; Published 19 July 2021

Academic Editor: Wei Wang

Indoor 3D positioning system requires precise information from all three dimensions in space, but measurements in the vertical direction are usually interfered by sensors properties, unexpected obstructions, and other factors. Thus, accuracy and robustness are not guaranteed. Aiming at this problem, we propose a novel sensor fusion algorithm to improve the height estimation for a UWB-barometer integrated positioning system by introducing a pseudo reference update mechanism and the extended Kalman filter (EKF). The proposed fusion approach effectively helps with sensing noise reduction and outlier restraint. The results from numerical experiment investigations demonstrate that the accuracy and robustness of the proposed method achieved better improvement in height determination.

1. Introduction

With mobile networks' development, people's demand for positioning and navigation has increased rapidly, especially in industrial applications with complex indoor facilities, such as intelligent power supply stations, urban underground trenches, and petrochemical plants [1]. Therefore, it has definite practical meaning to perform real-time location monitoring and tracking for moving targets in these scenarios. At present, ultra-wideband (UWB) network, radio frequency identification technology, and laser scanner are popular methods that provide indoor position information [2–5]. The UWB has high accuracy, strong stability, good antimultipath effect, low transmitting power, and low radiation [6]. Theoretically, such advantages make it capable of acquiring high precision three-dimensional position information in a spacious place. However, there are many occlusions in natural industrial environments, and the inside elevation is usually limited. These existing factors block the UWB signal in the vertical direction and significantly reduce height estimation accuracy [7].

Different from the UWB network, a barometer does not render three-dimensional location information. It only determines elevation through differential pressure calculation and is widely used for outdoor field applications [8]. If this barometer feature can be applied to UWB localization, it will be an excellent complement. Barometers' working manner has no defective impact on the UWB network. Moreover, its height estimates can make up when UWB failed to fetch height information and improve system sensing reliability [9, 10]. Usually, people first calibrate barometers to the value of mean sea level [11]. However, unlike outdoor sensing, the atmosphere inside a room changes little regarding the absolute sea-level reference raising another challenge. One of

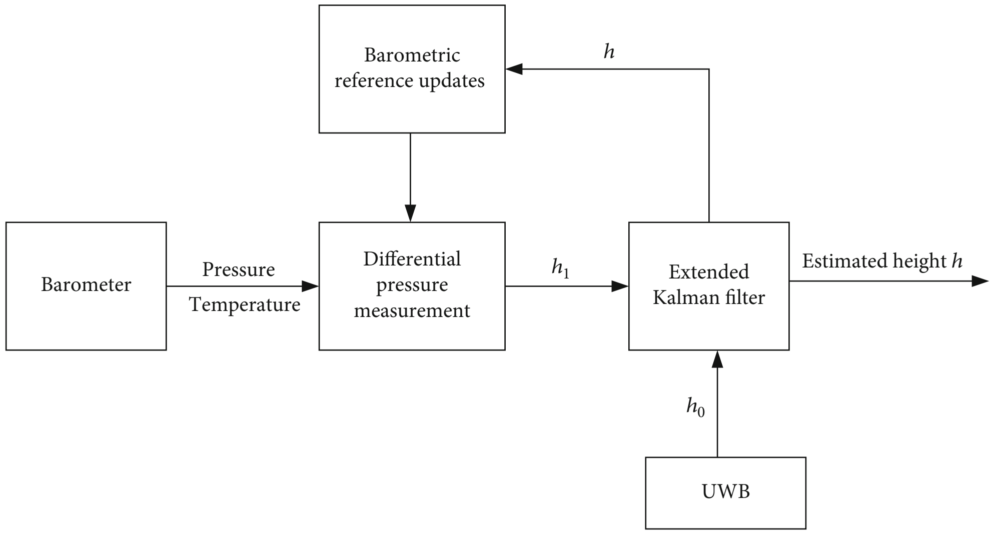

Figure 1: Sensing system overview.

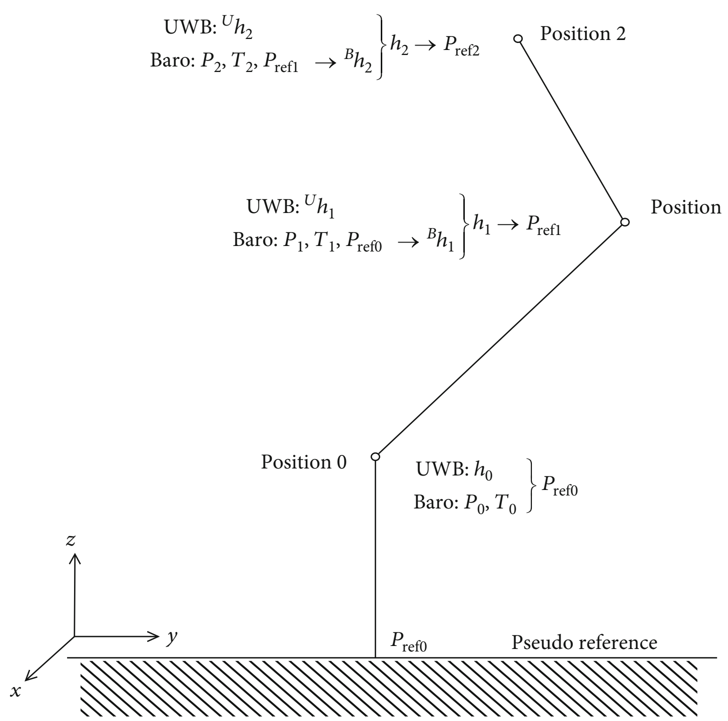

Figure 2: Pseudoreference updates.

the solutions is to set up a new pressure reference, then conduct differential pressure measurements based on this reference [12–14].

Many works have been done on this topic. Using differential calculation by two barometric sensors can make forecasted data more accurate [15, 16]. However, using two barometric sensors for differential calculation also has some disadvantages. For instance, barometric sensors require effective and frequent calibration to avoid long-term drifts, which affects the final height estimation accuracy [17]. Thus, height estimation's long-term accuracy and stability relying on individual pressure sensors are poor [18]. Considering these shortcomings of a single technology, supplementing various measurement advantages can achieve better position accuracy. The vertical height is underestimated due to the nonlinearity caused by the downward integration of the rotating accelerometer [19]. However, extended Kalman filter (EKF) can be used to apply the nonlinear Gaussian distribution [20], then joint EKF can deal with the nonlinearity problem to stabilize the height estimate.

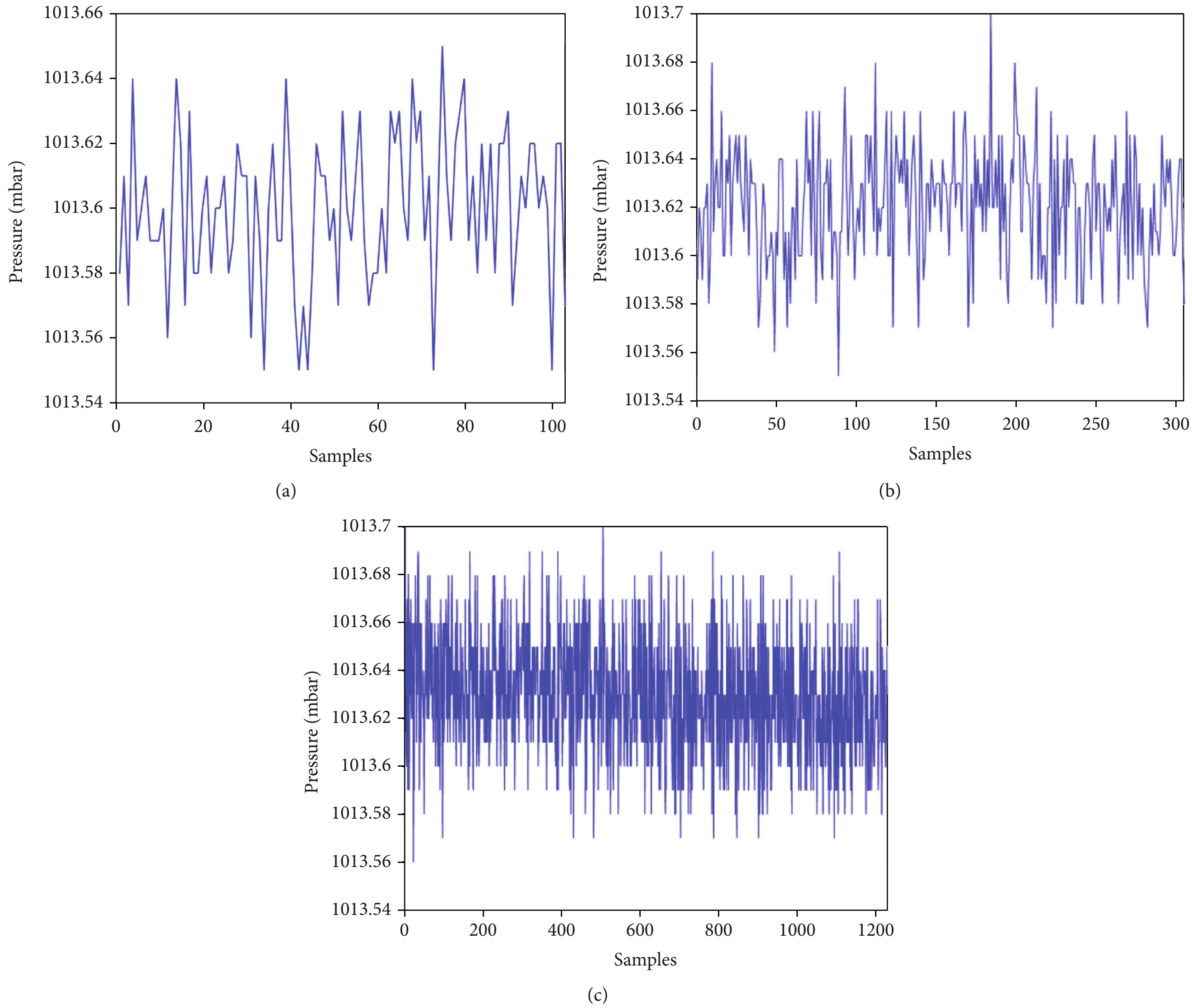

Figure 3: Static measured pressure with barometer for different durations. (a) Time duration is 10 seconds, (b) time duration is 30 seconds, and (c) time duration is 120 seconds.

The main contributions in this paper are as follows.

To improve accuracy and robustness for indoor height estimation, we propose a barometer-integrated UWB height estimation method. The proposed method has greatly improved the accuracy and stability of the estimated height.

During the height estimation, a pseudopressure reference update mechanism is proposed, and the scheme enables the barometer to achieve better performance in indoor environments.

The remainder of this article is organized as follows. The proposed barometer-integrated UWB height estimation method is depicted in Section 2. Section 3 illustrates the experiment's analyses and results. Section 4 shows conclusions.

2. Proposed Method for Height Estimation

Beacons in the 3D positioning system are installed on the floor and ceil two layers. Positioning can be achieved by sampling the selected beacons. However, when the elevation difference is limited and the floor beacons are blocked, the fluctuation of elevation estimation is relatively large. It is not easy to distinguish the upper and lower base stations on some occasions, so that the height estimation cannot be determined. Meanwhile, higher accuracy can be achieved for a reasonable open topological structure. Once occurring, outliers bring a tremendous challenge for positioning.

Table 1: Static barometer reading average and standard deviation in 10 s, 30 s, and 120 s.

Period	10 s	30 s	120 s
Ave (mbar)	1013.600	1013.621	1013.630
Std (mbar)	0.0231	0.0238	0.0243

Decimeter level altitude estimation can be gained through the double barometer differential method when high precision air pressure sensors are adopted. However, the

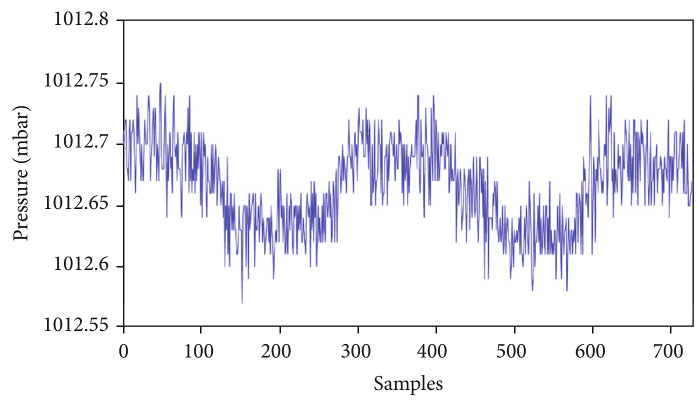

Figure 4: Measured pressure for barometer moving up and down within 50 cm.

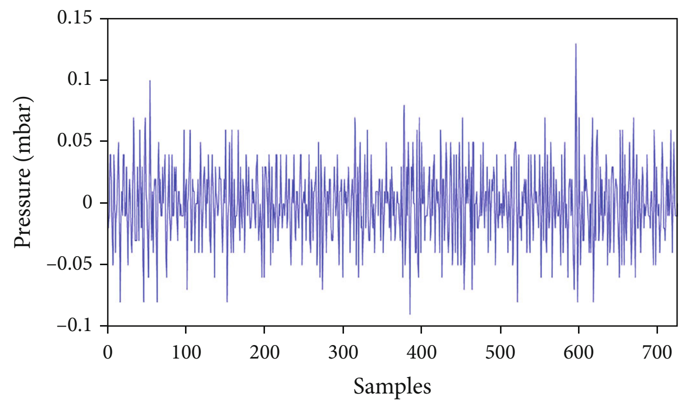

Figure 5: Pressure difference between two adjacent pressures.

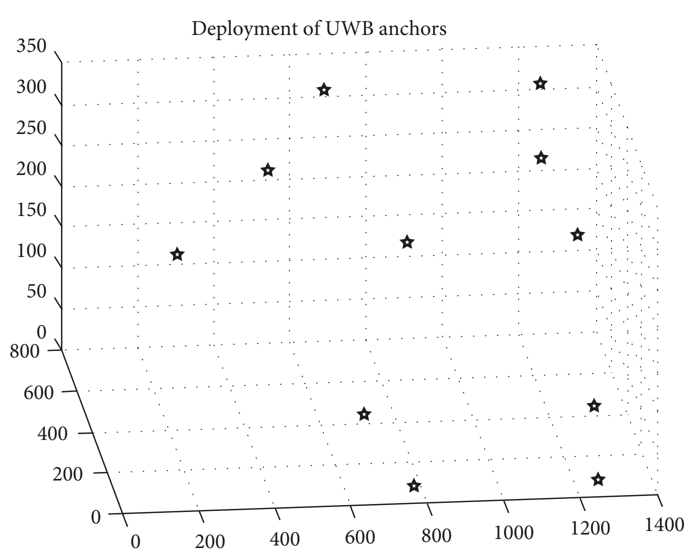

Figure 6: The deployment of 11 UWB anchors in the room with $14 * 8 * 3.5\,\text{m}^3$.

pressure deviation between barometers is not stable for a long time, so the deviations between barometers need to be corrected at intervals.

UWB signal has strong penetration ability and good anti-multipath performance, especially in indoor or building intensive environments. It can avoid the shielding effect, and the short-term stability of the barometric pressure sensor can benefit to assist the height estimation.

Aiming to improve the accuracy and reliability of measurement in a vertical direction, a novel high-precision

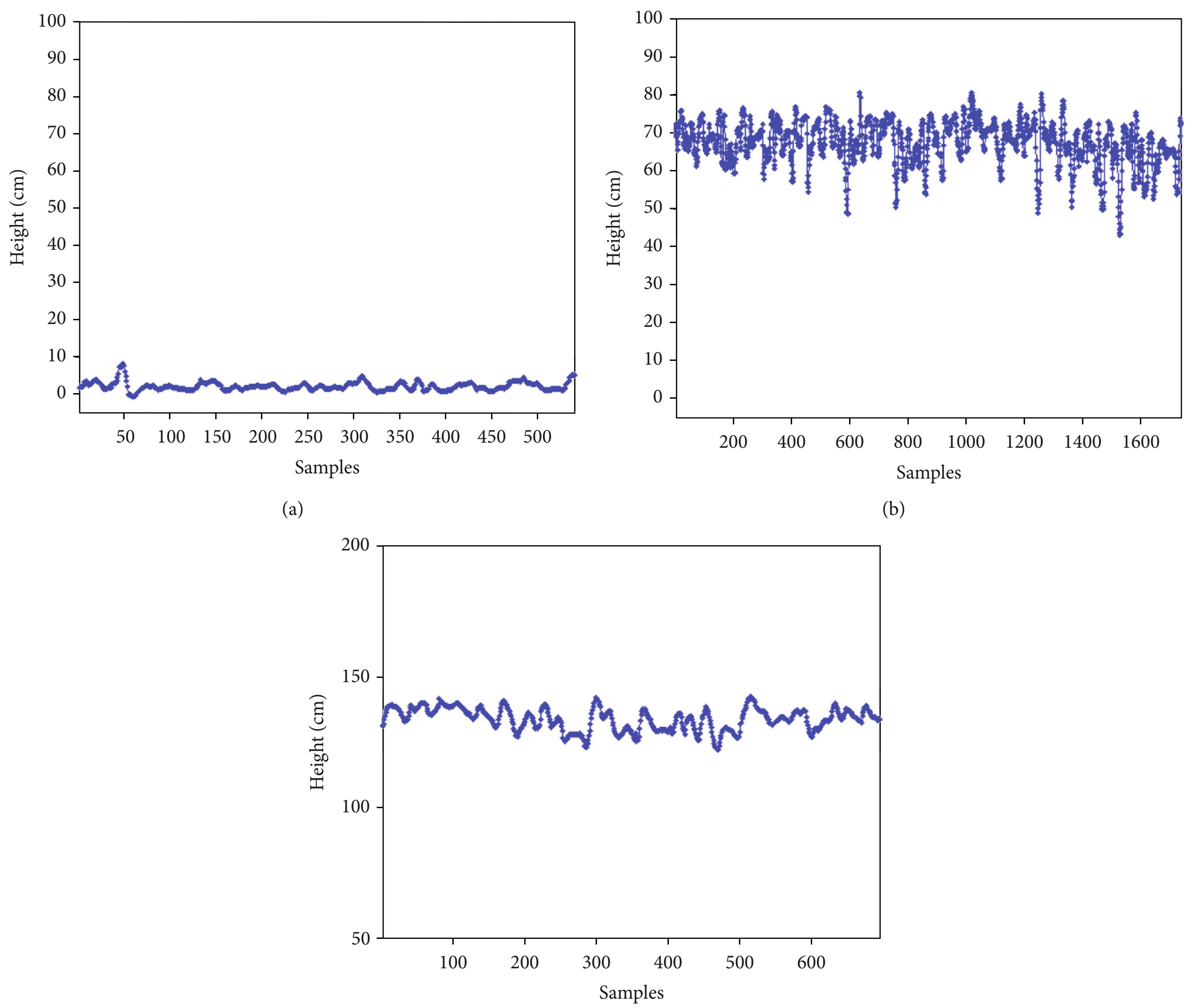

Figure 7: The estimated height with UWB anchors at different heights: (a) height = 0 cm, (b) height = 76 cm, and (c) height = 150 cm.

three-dimensional positioning method based on the fusion of ultrawideband and barometric pressure sensors is proposed. In the proposed method, the single barometer is adopted to eliminate device differences. In this section, we first introduce the general mechanism of EKF, then we describe how the barometer reference update and data fuse in the proposed method, as illustrated in Figure 1.

2.1. Extended Kalman Filter. EKF is used for nonlinear systems and noise models, which is a kind of the general Kalman filter (KF) [21]. In the EKF, the state transformation model and observation model are formulated by nonlinear functions. These two nonlinear models are described as state transition model:

$$x_k = f(x_{k-1}, u_{k\text{-}1}, s_{k\text{-}1}) \quad s_k \sim N(0, Q), \tag{1}$$

Table 2: Static barometer reading average and standard deviation at different heights.

Ground truth	0 cm	76 cm	150 cm
Ave (cm)	1.99	67.08	133.61
Std (cm)	1.15	5.75	4.25

and observation model:

$$z_k = w(x_k, v_k) \quad \sim v_k N(0, R), \tag{2}$$

where $f(\cdot)$ and $w(\cdot)$ are the nonlinear functions with x_{k-1}, u_{k-1}, s_{k-1}, and x_k, v_k, respectively. s_k is system process noise and zero-mean Gaussian process with covariance Q, and v_k is observation noise and zero-mean Gaussian process with covariance R. u_k denotes the input at time $k-1$. x_k and x_{k-1} represent the state variable at time k and $k-1$, respectively. z_k is the measurement at time k.

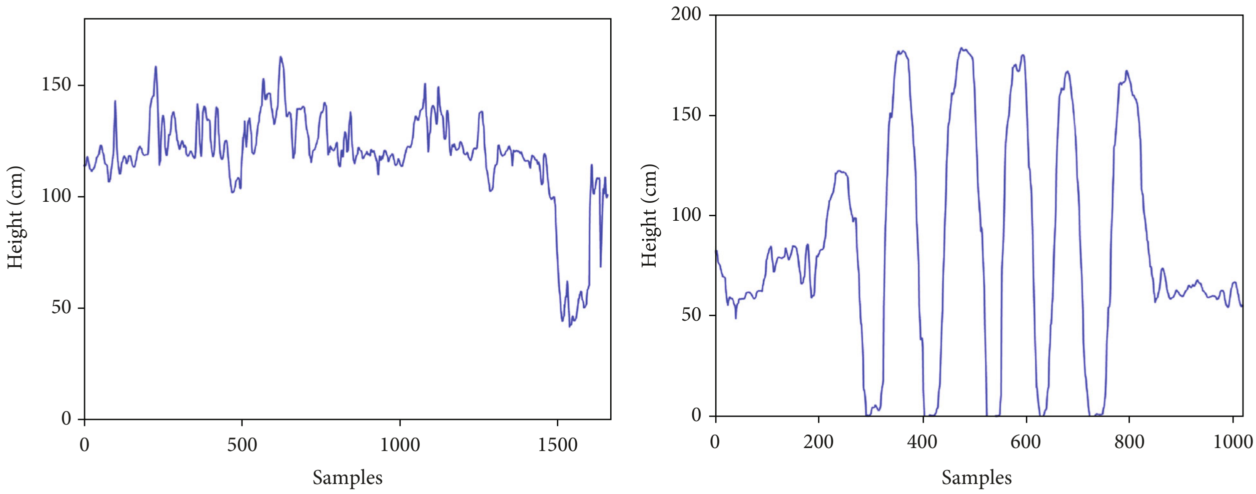

(a) (b)

Figure 8: The estimated height of moving target: (a) target move at 130 cm height and (b) target moves up and down.

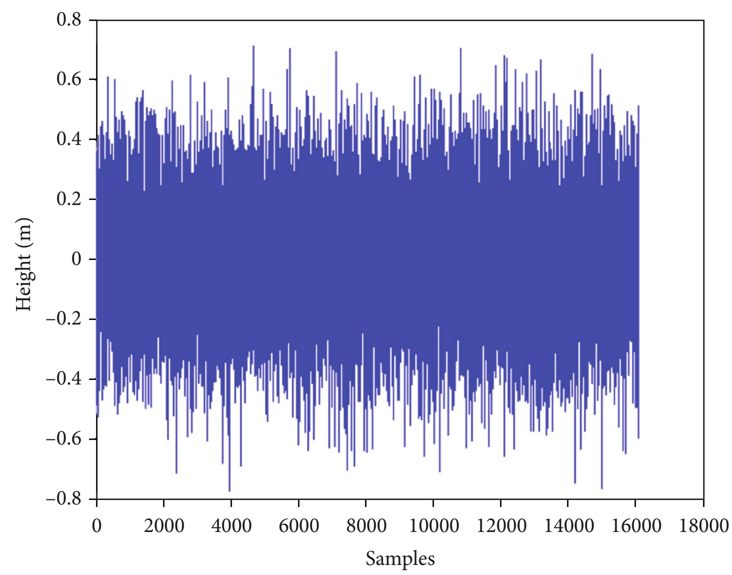

Figure 9: Simulated UWB data at 0 cm height.

Linearizing the two nonlinear Equations (1) and (2) by a first-order Taylor series approximation at $\widehat{x}_k$, then we get the linear equations as follows:

$$x_k = f(\widehat{x}_{k-1}, u_{k\text{-}1}, s_{k\text{-}1}) + F_{k-1}(x_{k-1} - \widehat{x}_{k-1}) + B_{k-1}s_{k-1}, \quad (3)$$

$$z_k = w(\widehat{x}_k, v_k) + W_k(x_k - \widehat{x}_k) + V_k v_k, \quad (4)$$

where F_{k-1} and $B_{k\text{-}1}$ are the Jacobian matrices of $f(\cdot)$ with respect to $\widehat{x}_{k\text{-}1}$ and s_{k-1}, and W_k and V_k are the Jacobian matrices of $w(\cdot)$ with respect to $\widehat{x}_k$ and v_k.

In the height estimation, we suppose the process noise is zero, therefore, $f(\widehat{x}_{k-1}, u_{k\text{-}1}, s_{k\text{-}1})$ in Equation (3) is the estimated value $\widehat{x}_k$ at time k. $w(\widehat{x}_k, v_k)$ in Equation (4) is the estimated value $\widehat{z}_k$ at time k. Substitute $\widehat{x}_k$ and $\widehat{z}_k$in the Equations (3) and (4), state transition model and observation model in the EKF can be expressed the linear function as follows:

$$x_k = \widehat{x}_k + F_{k-1}(x_{k-1} - \widehat{x}_{k-1}) + B_{k-1}s_{k-1}, \quad (5)$$

$$z_k = \widehat{z}_k + W_k(x_k - \widehat{x}_k) + V_k v_k. \quad (6)$$

EKF iterates in two major steps, the state prediction can be gained as Equations (7) and (8) and the state update as Equations (9) to (11).

$$\widehat{x}_{k|k-1} = f(\widehat{x}_{k-1}, u_{k\text{-}1}, 0), \quad (7)$$

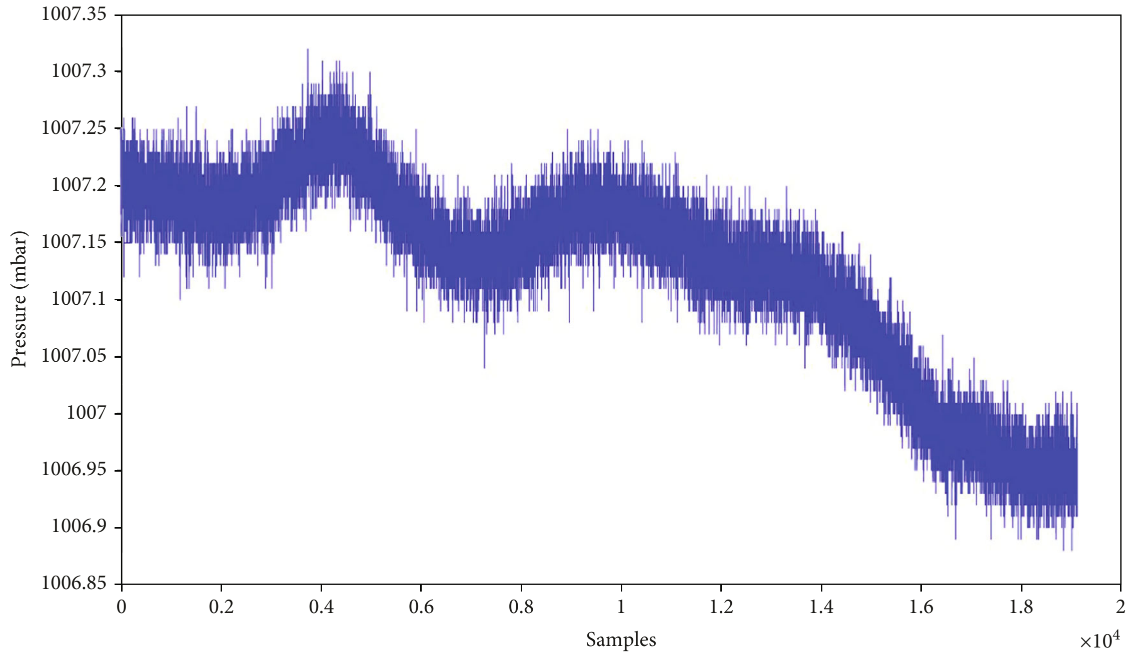

Figure 10: Measured pressure at 0 cm with barometer.

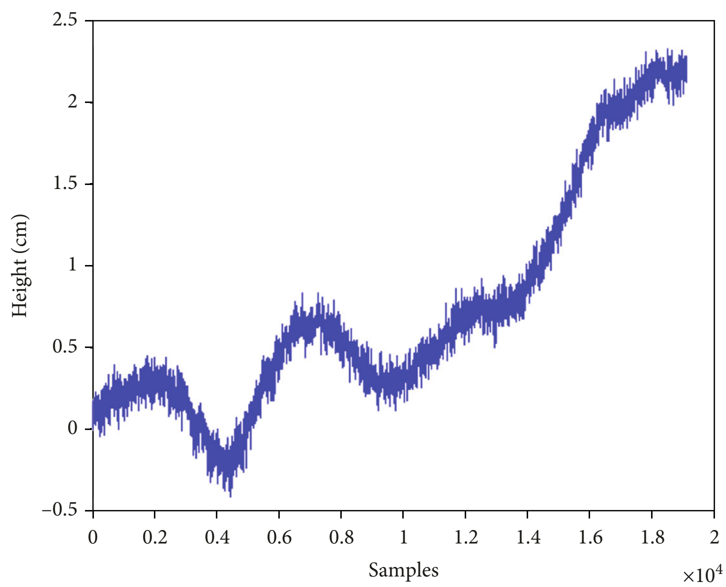

Figure 11: Estimated height with only barometer pressure sensor at 0 cm.

$$P_{k|k-1} = F_{k-1}P_{k-1}F_{k-1}{}^{T} + B_{k-1}QB_{k-1}{}^{T}. \quad (8)$$

In the prediction step, process noise is unknown, state prediction $\hat{x}_{k|k-1}$ is calculated by supposing s_k is zero. Its covariance $P_{k|k-1}$ at time k is calculated through Equations (8). Q denotes the estimated process noise covariance, which is fixed in the paper. In this paper, Q is the unit diagonal matrix.

$$K_k = P_{k|k-1}W^{T}\left(WP_{k|k-1}W^{T} + V_kRV_k\right)^{-1}, \quad (9)$$

$$\hat{x}_k = \hat{x}_{k|k-1} + K_k\left(z_k - W\left(\hat{x}_{k|k-1}, 0\right)\right), \quad (10)$$

$$P_k = (I - K_kW)P_{k|k-1}. \quad (11)$$

In the update step, the measurement at time k is taken into account. K_k is the Kalman gain, and it will converge as the filter iterates. Outputs of EKF are the optimal state $\hat{x}_k$ and its covariance P_k which will be considered as inputs of the next iteration. The estimated state $\hat{x}_k$ is the height h_k.

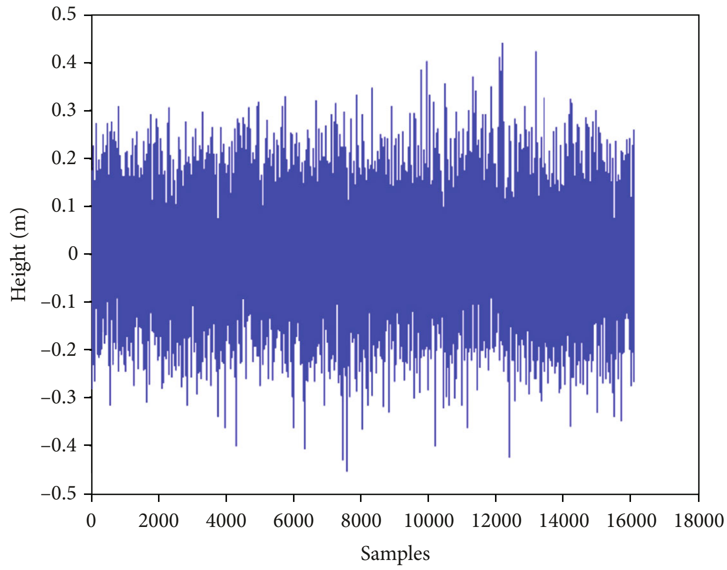

FIGURE 12: Estimated height at 0 cm with fusion UWB and barometric.

We deploy a barometer to estimate the system state relying on the nonlinear model as Equation (10) shows, and a UWB network to observe the system. Therefore, EKF is a feasible approach to handle this nonlinear-Gaussian fusion problem.

2.2. Pseudobarometeric Reference Establishment and Update. As we all know, the atmospheric pressure will decrease with the increase in altitude, and barometers can be used to obtain altitude information. However, barometers are plagued by an unpredicted environment whose accuracy could be at 0.5 m, but it can provide short-term stable measurement. By considering UWB and barometers' complementary features, a 4-step mechanism to establish and update barometric reference is realized in the paper as shown in Figure 2.

Step 1. Initialization: determine the first height h_0 by trilateration algorithm according to UWB anchors.

Step 2. Reference pressure establishment.

The pressure P_0 is determined from h_0. Reference pressure is updated through Equation (12).

$$P_{\mathrm{ref0}} = 10\wedge\left(\frac{h_0 - h_{\mathrm{ref}}}{18410} * \frac{273.15}{273.15 + T_0}\right) * P_0, \qquad (12)$$

where P_{ref0} is the calculated pressure at the pseudoreference level, and T_0 denotes the temperature at the initial measuring point, h_{ref} equals to zero.

Step 3. Height determination.

With the reference pressure P_{ref0}, the pressure P_1, and temperature T_1 measured by barometer at position 1, the estimated height ${}^{B}h_1$ can be determined through Equation (13). Here, the superscript letter B indicates estimation inferred by barometer data.

TABLE 3: Estimated height results at 0 cm.

Methods	UWB	Barometer	UWB-Baro-EKF(proposed)
Ave (cm)	0 (GT)	0.82	0.16
Std (cm)	20.06	14.42	10.69

$${}^{B}h_1 = 18410 * \left(1 + \frac{T}{273.15}\right) \lg \frac{P_{\mathrm{ref0}}}{P_1} + h_{\mathrm{ref}}, \qquad (13)$$

where T is an average of T_1 and T_0.

Step 4. Reference update.

At position 1, UWB determines a ${}^{U}h_1$ through trilateral calculation. By combining ${}^{U}h_1$ and ${}^{B}h_1$, the EKF outputs an optimal estimation height $\widehat{h}_1$ with covariance H_1. Similar to the process in step 2, we calibrate the reference pressure based on h_1 through Equation (9).

According to EKF theory, the accuracy of h_1 is higher than h_0, therefore, the updated reference pressure P_{ref1} is closer to its true value.

3. Experimental Results

The experiments are mainly conducted in three parts. In the first two parts, the stability and accuracy of the applied barometer and UWB are tested, then the proposed fusion method is tested in the last part.

3.1. Barometer. In the experiments, the barometric pressure sensor (Swiss) MS5611 is used to measure the air pressure and has a high-resolution barometric pressure sensor with SPI and I^2C bus interface introduced by MEAS (Switzerland).

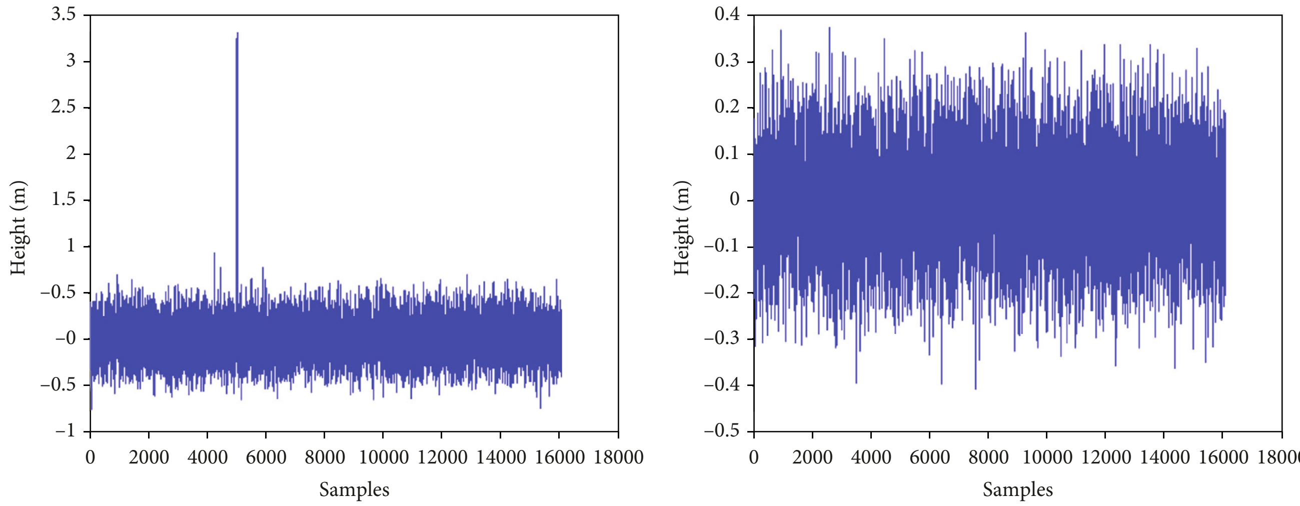

(a) UWB simulation dada generated with single outlier

(b) Estimated height with proposed method

Figure 13: Original UWB data with single outlier and estimated height with the proposed method.

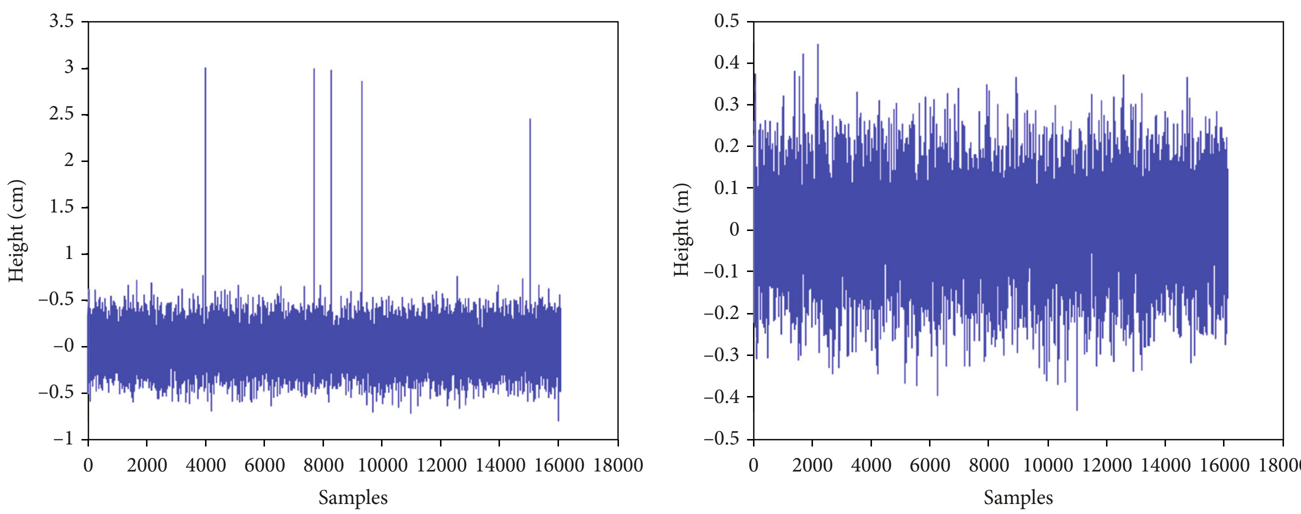

(a) UWB simulation dada generated with outliers

(b) Estimated height with the proposed method

Figure 14: Original UWB with outliers and estimated height with the proposed method.

First, we test the barometer's static measurement by setting it at a certain level and collect atmosphere pressure data in 10 s, 30 s, and 120 s shown in Figure 3. With measuring time increases from 10 seconds to 120 seconds, the range where data fluctuates becomes larger. Table 1 reflects the average measurements and standard deviations. There is only little figural change on moderate pressure, suggesting that the barometer can maintain short-term stability. For long-term measurement, a periodical calibration is required because readings begin to disperse after 40 seconds.

We also test the barometer's dynamic measurement by the 50 cm range vertical reciprocating movement. Figure 4 shows the measured pressure as the barometer moves up and down within 50 cm. Meanwhile, we do several times experiments continuously to sample pressure. Figure 5 depicted the pressure difference between two adjacent pressures. It can be seen that the barometer can effectively identify the up and down motion by measuring atmosphere pressure and also have better stability. Moreover, the feature of accordant pressure difference can help with outlier removal and data refinery.

3.2. UWB Height Estimation. To validate the location performance adopted by UWB, we conducted experiments on static and moving targets, respectively. An indoor UWB network with 11 anchors is installed in the room with $14 * 8 * 3.5\,m^3$. The anchor deployment is distributed as Figure 6.

Figure 7 shows the location results of static targets at 0 cm, 76 cm, and 150 cm heights, respectively. It is shown that the positioning results fluctuate around the real value, especially at the height of 76 cm, and the accuracy can reach decimeter level. When the static target is at 0 cm,

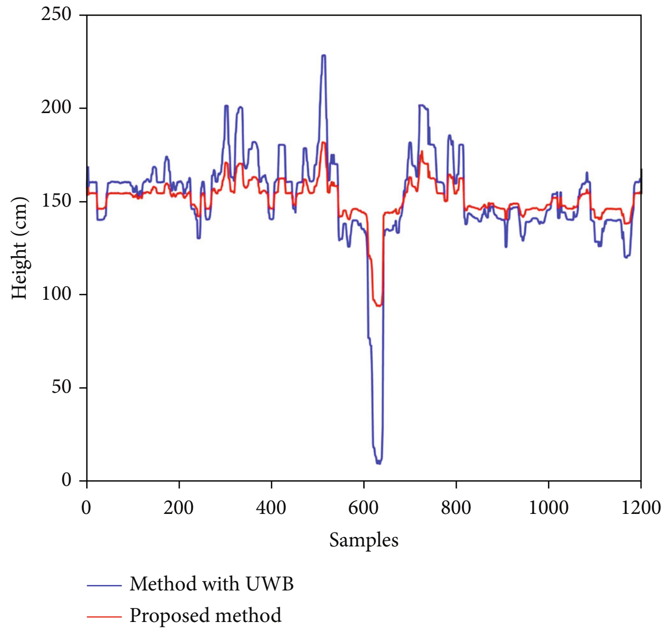

Figure 15: Height estimation between the proposed method and method with only UWB at 150 cm.

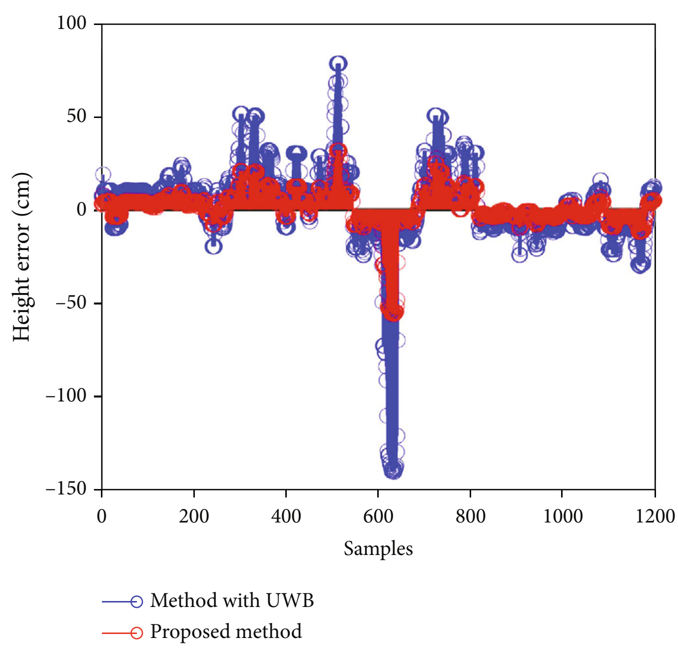

Figure 16: Height error between the proposed method and method with only UWB.

the estimated height error is 1.99 cm and variance is 1.15 cm. The estimated height error at 76 cm is 8.92 cm and its variance is 5.75 cm. When the target lies at 150 cm, the estimation height error is 16.39 cm and its variance is 4.25 cm. Table 2 depicted the estimated height and variance.

Meanwhile, two experiments for a moving target are conducted. One volunteer holds a tag at 130 cm height and walks around. Other volunteer holds the tag up and down. Figure 8 described the positioning results of the moving target. It is shown that the positioning accuracy reaches 30 cm with only receiving UWB signals when the anchors are installed in a reasonable and open topological environment.

Table 4: Estimated height results at 0 cm.

Methods	UWB	UWB-Baro-EKF (proposed)
Ave (cm)	151.77	150.677
Std (cm)	0.799	0.319

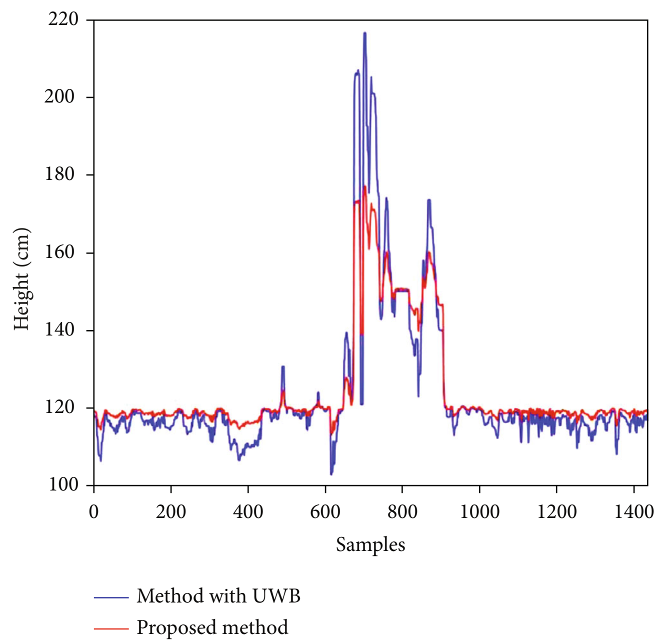

Figure 17: Height estimation between the proposed method and method with only UWB at different height locations.

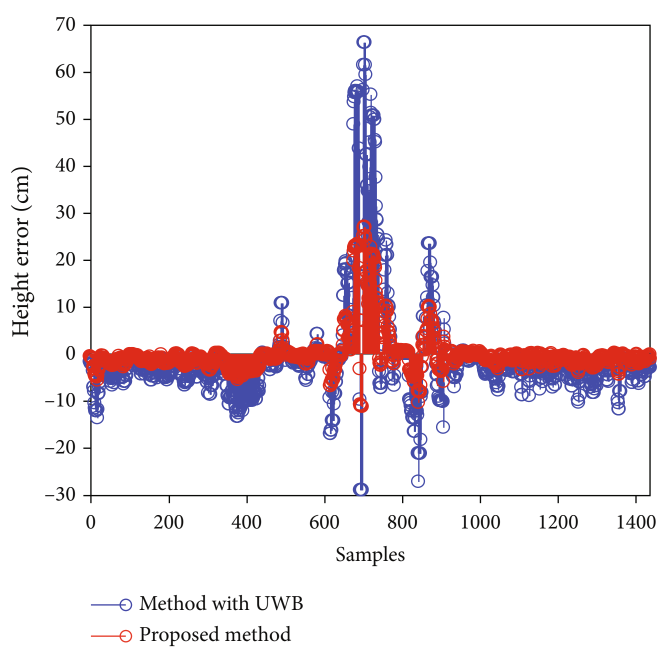

Figure 18: Height error between the proposed method and method with only UWB at different height locations.

However, when the target is located in an unreasonable topology, the estimated height will occur on outliers, especially for 1-2 meters shown in Figure 8. The estimated height only used UWB technology will be deteriorated.

3.3. Barometer-Assisted UWB Height Estimation. Assuming the simulated height estimates from UWB is a zero-mean Gaussian with standard deviation, we randomly generate the estimated height with zero-mean and 20.06 cm variance as shown in Figure 9. The barometric pressure sensor (Swiss) MS5611 is located at 0 cm height, and its measured data are shown in Figure 10. Figure 11 depicted the estimated height with only barometer pressure sensor.

Following the proposed pseudo reference update and EKF fusion, the standard deviation of estimated height reduces from 20.06 cm to 10.69 cm as Figure 12. Table 3 includes the results of all three sets, indicating the significant accuracy improvement.

In the robustness test, we consider errors over 1 m from single sensor as outliers and add such outliers randomly into

UWB simulation data. Figure 13(a) shows the UWB data with single outlier. Figure 13(b) shows the estimated height result with our proposed method. Figure 14(a) shows the UWB data with synthetic outliers. Figure 14(b) shows the estimated height result with our proposed method. It is evident that output data are more concentrated, and outliers are restrained.

Experiments show that the proposed method improved the height estimation performance and solved the problem that height positioning cannot be realized on some occasions. The short-term stability of barometer is fully utilized to assist UWB height estimation. Our method can suppress the abnormal value of height estimation in pure ultrawideband three-dimensional positioning, whether it is an isolated outlier or a continuous outlier. The requirement for frequent calibration of two differential pressure stations in traditional differential altimetry is avoided.

In addition, to verify the effectiveness of the fusion algorithm in the actual environment, the target located in the same height and different heights, respectively, are tested. First, the target is located at 150 cm in height. The height estimation and error are shown in Figures 15 and 16.

Figure 15 demonstrates that the positioning accuracy adopted by the proposed method is more improved than the single UWB method. When the samples are about 650, continuous outliers appear in UWB, and the proposed method can effectively restrain the outliers. Figure 16 shows the height errors between the proposed method and the single UWB method.

Table 4 depicts the average estimated height and variance with the proposed method and only UWB.

We also test the different heights of the target experiments. First, the target is installed at 120 cm, then walking by hand at 150 cm height, and then placed at 120 cm. The height estimation and error in a state of moving are shown in Figures 17 and 18.

The results show that the height accuracy of the proposed methods is better when the target is located in the same high position. However, when the target transfers from one altitude to another, the positioning accuracy will deteriorate, and outliers will appear with only UWB technology. Through the proposed method, the height estimation can keep up with the target position. The proposed method has better performance than the single UWB method.

4. Conclusions

This paper proposes an altitude estimation method, which is composed of UWB system and barometers. It can make a reliable and accurate estimation. In this paper, some experiments' data have proved that this method can enhance height direction measurement accuracy. In addition, a dynamic indoor pressure reference is taken into account and has been proven capable of providing more accurate sensing in complex indoor situations. The improved robustness of the EKF also has some limitations. However, it is still crucial to reliably detect and remove outliers from UWB raw data.

Data Availability

After discussion between all authors, the experimental data are temporarily unavailable. If readers want to study this field further, readers can ask the author for data.

Conflicts of Interest

The authors declare that they have no conflicts of interest.

Acknowledgments

This work was partially supported by the National Natural Science Foundation of China (Nos. 61772149, 61936002, 2018AAA0100300, 6202780103, 62033001, and 62061010) and Guangxi Science and Technology Project (Nos. AD18216004, AA18118039, 2019GXNSFFA245014, 2019GXNSFBA245072, and AD18281079).

References

[1] A. Zhen-Peng, S. Hu-Lin, and W. Jun, "Classify and prospect of indoor positioning and indoor navigation," in *2015 Fifth International Conference on Instrumentation and Measurement, Computer, Communication and Control (IMCCC)*, pp. 1893–1897, Qinhuangdao, China, 2015.

[2] Z. Sahinoglu, S. Gezici, and I. Guvenc, *Ultra-Wideband Positioning Systems: Theoretical Limits, Ranging Algorithms, and Protocols*, Cambridge University Press, 2008.

[3] Y. Wu, S. Ding, Y. Ding, and M. Li, "UWB base station cluster localization for unmanned ground vehicle guidance," *Mathematical Problems in Engineering*, vol. 2021, Article ID 6639574, 23 pages, 2021.

[4] A. Ren, F. Zhou, A. Rahman, X. Wang, N. Zhao, and X. Yang, "A study of indoor positioning based on UWB base-station configurations," in *2017 IEEE 2nd Advanced Information Technology, Electronic and Automation Control Conference (IAEAC)*, pp. 1939–1943, Chongqing, China, 2017.

[5] V. Renaudin, M. Ortiz, J. Perul et al., "Evaluating indoor positioning systems in a shopping mall: the lessons learned from the IPIN 2018 competition," *IEEE Access*, vol. 7, pp. 148594–148628, 2019.

[6] J. D. Hoi, F. Dijkstra, H. Luinge, and T. B. Schon, "Tightly coupled UWB/IMU pose estimation," in *2009 IEEE International Conference on Ultra-Wideband*, pp. 688–692, Vancouver, BC, Canada, 2009.

[7] Q. Fan, Y. Wu, J. Hui, L. Wu, Z. Yu, and L. Zhou, "Integrated navigation fusion strategy of INS/UWB for indoor carrier attitude angle and position synchronous tracking," *The Scientific World Journal*, vol. 2014, Article ID 215303, 13 pages, 2014.

[8] Y. Son and S. Oh, "A barometer-IMU fusion method for vertical velocity and height estimation," in *2015 IEEE SENSORS*, pp. 1–4, Busan, Korea (South), 2015.

[9] R. Elbakly, M. Elhamshary, and M. Youssef, "HyRise," *Proceedings of the ACM on interactive, mobile, wearable and ubiquitous technologies*, vol. 2, no. 3, pp. 1–23, 2018.

[10] K. Muralidharan, A. J. Khan, A. Misra, R. K. Balan, and S. Agarwal, "Barometric phone sensors: more hype than hope!," in *Proceedings of the 15th workshop on mobile computing systems and applications*, pp. 1–6, Santa Barbara, California, 2014.

[11] B. Li, B. Harvey, and T. Gallagher, "Using barometers to determine the height for indoor positioning," in *International Conference on Indoor Positioning and Indoor Navigation*, pp. 1–7, Montbeliard, France, 2013.

[12] Z. Xu, J. Wei, J. Zhu, and W. Yang, "A robust floor localization method using inertial and barometer measurements," in *2017 International Conference on Indoor Positioning and Indoor Navigation (IPIN)*, pp. 1–8, Sapporo, Japan, 2017.

[13] V. Chueh, T. Li, and R. Grethel, "INS/Baro vertical channel performance using improved pressure altitude as a reference," in *2008 IEEE/ION Position, Location and Navigation Symposium*, pp. 1199–1202, Monterey, CA, USA, 2008.

[14] H. Ye, T. Gu, X. Tao, and J. Lu, "SBC: scalable smartphone barometer calibration through crowdsourcing," in *Proceedings of the 11th International Conference on Mobile and Ubiquitous Systems: Computing, Networking and Services*, pp. 60–69, London, Great Britain, 2014.

[15] M. Tanigawa, H. Luinge, L. Schipper, and P. Slycke, "Drift-free dynamic height sensor using MEMS IMU aided by MEMS pressure sensor," in *2008 5th Workshop on Positioning, Navigation and Communication*, pp. 191–196, Hannover, Germany, 2008.

[16] D. E. Bolanakis, "Evaluating performance of MEMS barometric sensors in differential altimetry systems," *IEEE Aerospace and Electronic Systems Magazine*, vol. 32, no. 9, pp. 34–39, 2017.

[17] S. Hyuga, M. Ito, M. Iwai, and K. Sezaki, "Estimate a user's location using smartphone's barometer on a subway," in *Proceedings of the 5th International Workshop on Mobile Entity Localization and Tracking in GPS-less Environments*, pp. 1–4, Seattle, Washington, 2015.

[18] D. E. Bolanakis, K. T. Kotsis, and T. Laopoulos, "A prototype wireless sensor network system for a comparative evaluation of differential and absolute barometric altimetry," *IEEE Aerospace and Electronic Systems Magazine*, vol. 30, no. 11, pp. 20–28, 2015.

[19] D. Banerjee, S. K. Agarwal, and P. Sharma, "Improving floor localization accuracy in 3D spaces using barometer," in *Proceedings of the 2015 ACM International Symposium on Wearable Computers - ISWC '15*, pp. 171–178, Osaka, Japan, 2015.

[20] Y. Xu, G. Tian, and X. Chen, "Performance enhancement for INS/UWB integrated indoor tracking using distributed iterated extended Kalman filter," in *2018 Ubiquitous Positioning, Indoor Navigation and Location-Based Services (UPINLBS)*, pp. 1–5, Wuhan, China, 2018.

[21] R. E. Kalman, "A new approach to linear filtering and prediction problems," *Journal of Basic Engineering*, vol. 82, no. 1, pp. 35–45, 1960.